ELSEVIER

Journal of Nuclear Materials 266–269 (1999) 867–872

journal of nuclear materials

Modelling of deuterium emission in high density divertor plasmas in JET

C.F. Maggi [a,*], L.D. Horton [a], G. Corrigan [a], H.J. Jäckel [a], A. Loarte [b], R.D. Monk [a], R. Simonini [a], M. Stamp [a], A. Taroni [a]

[a] *JET Joint Undertaking, Abingdon, OXON, OX14 3EA, UK*
[b] *The NET Team, Max Planck Institut für Plasmaphysik, D-85748 Garching, Germany*

Abstract

Simulations of neutral deuterium emission from high density Ohmic and L-mode JET divertor discharges with the EDGE2D/NIMBUS codes are presented. At high density the codes fail to reproduce quantitatively the steady increase of divertor D^0 emission with rising plasma density observed in the experiment. However, good agreement is obtained with the measured D_γ/D_α ratio in inner and outer divertor despite the total plasma volume recombination being small in the simulations. The asymmetry between inner and outer divertor detachment is found to depend on the strength of the charge exchange momentum losses. Recombination alone is not sufficient to obtain strong detachment in the inner divertor. Measurements of Ly_β/D_α emission profiles across the JET divertor show signs of Lyman radiation reabsorption in the inner divertor at high density. The first attempt at including divertor plasma opacity corrections self-consistently in EDGE2D/NIMBUS simulations of high density JET L-mode discharges is presented. The effect of opacity on the simulated deuterium emission and on the 2D plasma solution is discussed.

Keywords: JET; Deuterium emission; Divertor modeling

1. Introduction

Modelling neutral deuterium emission from high density divertor plasmas is of particular interest because it contains information on the recycling patterns, the balance between ionization and recombination and the opacity of the divertor plasma.

This paper presents the latest results in this area for the simulation of JET Ohmic and L-mode discharges using the 2D fluid/Monte Carlo EDGE2D/NIMBUS [1] codes.

2. Spectroscopic observations

In Ohmic and L-mode density limit (DL) discharges neutral deuterium emission from the divertor region of JET is measured by visible and VUV spectroscopy [2] to increase continuously with rising main plasma density. In the MarkIIA divertor, more closed to recycling neutrals than the previous MarkI geometry [3], the deuterium line emission is higher than in MarkI for the same plasma density. This is illustrated in Fig. 1 for similar L-mode DL discharges with vertical target configuration (i.e. with the strike zones on the divertor side plates). A smaller increase in D_α emission from MarkI to MarkIIA is observed in Ohmic and L-mode DL discharges with horizontal target configuration.

Measurements of D^0 Lyman-β (Ly_β) and Balmer-α (D_α) profiles across the divertor in MarkIIA show signs of Lyman radiation reabsorption in the inner divertor leg at high density, with a decrease in Ly_β/D_α ratio of order 30%. One such example is shown in Fig. 2 at three subsequent times during a high density, quasi-steady ELMy H-mode discharge (the measurements are taken in between the type I ELMs). These profile measurements were obtained with a VUV duochromator equipped with a rotating mirror (for Ly_β) and with a CCD camera with interference filter (for D_α). Both

* Corresponding author. Tel.: +44 1235 465 335; fax: +44 1235 464 535; e-mail: costanza.maggi@jet.uk

0022-3115/99/$ – see front matter
PII: S0022-3115(98)00845-9

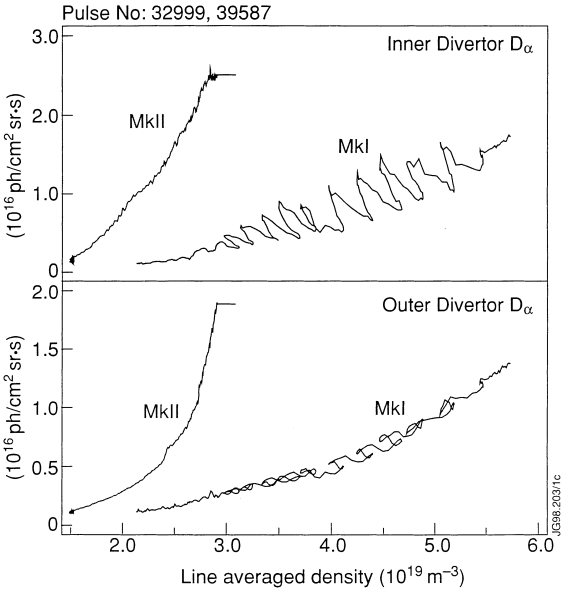

Fig. 1. D_α emission from inner and outer divertor versus central line averaged electron density in two similar L-mode DL discharges in MarkI and MarkIIA with vertical target configuration. The D_α signal saturates before the density limit in the MarkIIA discharge.

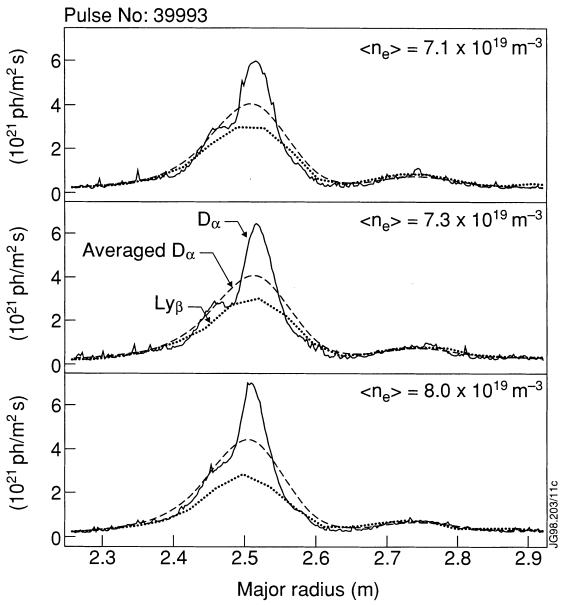

Fig. 2. Deuterium Ly_β and D_α emission profiles across the divertor measured at three different times in a high density quasi-steady ELMy H-mode discharge in MarkIIA (profiles measured during ELM-free periods) showing signatures of Ly_β reabsorption in the inner divertor. The measured D_α profile (solid trace) is averaged over the VUV spectrometer spatial resolution (long-dashed trace).

systems look at the divertor target from the top of the JET tokamak. Since the CCD camera has a better spatial resolution at the divertor than the VUV spectrometer, the D_α emission profile has been averaged accordingly (see Fig. 2). Ly_β/D_α measurements in MarkI DL discharges, reported in Ref. [4], obtained along a fixed line-of-sight directed at the inner target, showed similar values of Lyman radiation reabsorption in the high density phase of such discharges (Ly_β/D_α ratio decreasing by 30–40% at high density).

3. 2D numerical simulations

Ohmic and L-mode DL discharges are simulated by performing density scans with the 2D EDGE2D/NIMBUS codes. The approach to detachment and to the DL is sought with a series of runs to steady state in which the upstream separatrix density (n_s) is progressively increased, while all other parameters are fixed. Constant perpendicular transport coefficients are used: $D_\perp = 0.1$ m^2 s^{-1} and $\chi_{e\perp} = \chi_{i\perp} = 1.5$ m^2 s^{-1}.

3.1. MarkI vs. MarkIIA geometry (pure plasma simulations)

Two similar L-mode DL discharges with vertical target configuration, one in MarkI and one in MarkIIA, are simulated with pure plasma only due to restrictions on CPU time (the simulations with impurities are in progress). The total input power crossing the separatrix is 2 MW and is split equally between electron and ion channels. For the same upstream separatrix density, the divertor neutral density is found to be higher in the more closed MarkIIA geometry simulations. This is consistent with experimental measurements which show improved pumping in MarkIIA [5] and is a direct consequence of improved divertor closure.

In the present version of EDGE2D/NIMBUS the calculation of ion momentum losses due to ion-neutral charge exchange (cx) collisions is performed after distinguishing between before ($v_0 = 0$, stationary neutrals) and after ($v_0 = v_i$, neutrals thermalized to plasma ions) the first cx event for a given neutral trajectory. This approximation yields almost symmetrical detachment between inner and outer divertor legs (Fig. 3(b)) contrary to experiment (Fig. 3(a)). In Fig. 3 we compare plasma detachment in different discharges using the 'degree of detachment' (DOD) as defined in Ref. [6], that is the inverse ratio of the measured ion flux to the target to that expected in a high recycling divertor:

$$\mathrm{DOD} = \frac{Cn_e^2}{I_t^{\mathrm{meas}}}, \tag{3.1}$$

where I_t^{meas} is the measured ion flux to the target, n_e the central line averaged density and C a normalization

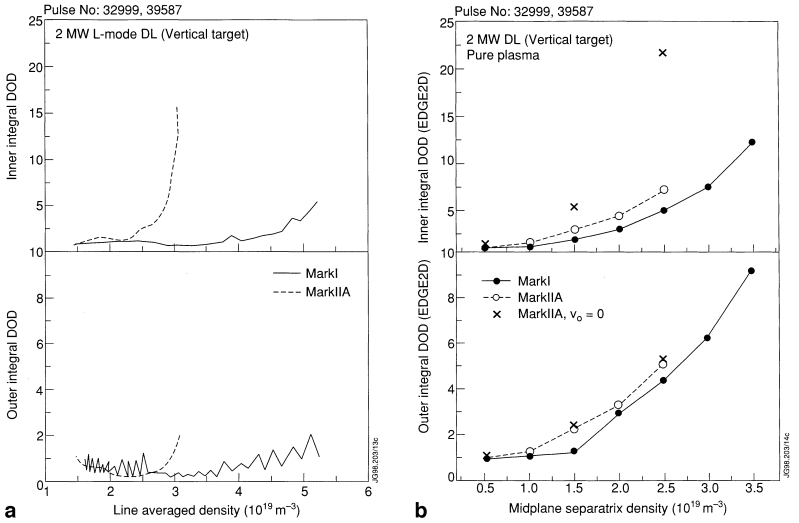

Fig. 3. (a) Experimental inner and outer divertor integral DOD for similar L-mode DL discharges on the vertical target in MarkI and MarkIIA versus central line averaged density. (b) Inner and outer divertor integral DOD from EDGE2D/NIMBUS pure plasma simulations of the discharges of Fig. 3(a) versus upstream separatrix density. The crosses denote the MarkIIA simulations with the assumption of stationary neutrals, $v_0 = 0$, in the calculation of cx ion momentum losses.

constant, obtained at low density where the DOD is defined to be 1. For the code results the DOD is derived using the upstream separatrix density and the calculated ion flux to the target. Note that the maximum value of the experimental DOD for the MarkI discharge (Fig. 3(a)) is underestimated due to the fact that strike point sweeping was used, which results in full ion flux profiles every 1/4 s.

Although comparable values of DOD are reached, the approach to detachment is qualitatively different in experiment (sharp increase of the DOD close to the density limit) and simulations (more gradual and steady increase of the DOD with density). In fact, whereas experimentally the total ion flux to the divertor target first rises and then falls rapidly as the density is increased, in the simulations a significant drop of ion flux after roll-over is not obtained with this assumption on the cx momentum losses. This result is a common feature of the simulations, both with pure plasma only and with impurities. In contrast, if all neutrals are assumed to be stationary ($v_0 = 0$) in the calculation of the cx momentum losses, which constitutes the upper bound ion momentum removal per cx collision, the asymmetry between inner and outer divertor detachment found in experiment is qualitatively reproduced by the code (Fig. 3(b), MarkIIA case, crosses). The simulations with the actual v_0 as computed in the Monte Carlo code are at present numerically unstable and thus cannot be compared. Work is in progress to overcome these difficulties.

The maximum upstream separatrix density obtained in the simulations is limited by the onset of a 'Marfe-ing' behaviour, with strong ionization above the X-point and cooling of the edge plasma, which eventually makes the solution unstable. This defines the density limit in the simulations. The density limit is reduced from MarkI to MarkIIA (Fig. 3(b)), although not by the same amount as in the experiment. However, this may just be a feature of the pure plasma simulations and a quantitative comparison of code results and experimental measurements can only be made once the full plasma/impurity simulations are available.

In the simulations, at the density limit the ratio of total (i.e. integrated over the whole plasma) recombination to ionization events is $f_{\mathrm{rec}} \sim 20\%$, with $f_{\mathrm{rec}} \sim 100\%$ in the inner and 10% in the outer divertor region separately, while the total ion flux to the divertor target is just starting to roll-over. The lack of reduction in total ion flux to the inner target despite strong local volume recombination in the inner divertor region is due to the strong ion flow in the inner scrape-off-layer. Borrass et al. [7] define 'complete divertor detachment' as a substantial drop of total ion flux to the target from its peak value, which is obtained in their pure plasma simulations only for $f_{\mathrm{rec}} \geqslant 60\%$ in the inboard side of the plasma. With this definition, the present EDGE2D solutions are only 'partially detached'. In the MarkIIA high density simulation with strong cx momentum losses (i.e. when $v_0 = 0$ is assumed), f_{rec} drops from $\sim$100% to $\sim$40% in the inner divertor, but reduction in total ion flux to the inner target from the peak value is achieved. This is shown in Fig. 3(b) by the increased inner integral DOD.

These tests on different assumptions on the strength of the cx momentum losses seem to indicate that strong

volume recombination alone is not sufficient to produce complete divertor detachment, but that it must be accompanied by strong enough charge exchange ion momentum removal. Also, the asymmetry between inner and outer divertor detachment depends on the assumptions made in the calculation of the cx momentum losses. These conclusions also apply to simulations with carbon impurities.

3.2. Simulations of a MarkIIA Ohmic DL discharge (with carbon impurities)

In the detailed simulation of a specific JET divertor discharge there are two free parameters: the ratio of separatrix to core line averaged density, $n_s/\langle n_e\rangle$, since the separatrix density is not routinely measured, and the chemical sputtering yield, Y_{chem}, which is not known with acceptable accuracy. Fig. 4 shows time traces of an Ohmic DL discharge in MarkIIA with vertical target configuration. Taking $n_s/\langle n_e\rangle = 0.6$ and $Y_{chem} = 2\%$ matches the total radiated power, P_{RAD}, at the highest density (Fig. 4, the results of the simulations are marked by crosses). The integral C III visible line emission ($\lambda = 4650$ Å) from inner and outer divertor is also reasonably well reproduced (not shown). The shape of the ion flux profiles measured at the divertor targets by Langmuir probes is well reproduced with the transport coefficients reported above. However, the integral ion flux to the inner divertor target is a factor of two higher than measured experimentally at high density, leading to a lower DOD in the simulations. In addition, as described in the previous section, inner and outer divertor detachment is symmetric in the code, contrary to experiment. $E \times B$ drifts, which may contribute to the asymmetry between inner and outer divertor detachment [8], are not included in these simulations.

The integral D^0 line emission (D_α, D_γ) from inner and outer divertor, well reproduced at the lower densities, does not show the strong increase with density seen in experiment and is underestimated by a factor of ~3 at the highest density (Fig. 4). In the high density simulation the contribution of recombination to the total emission is $I^{rec}/I^{tot} = 20\%$ (7%) for D_α and 62% (32%) for D_γ in the inner (outer) divertor. The rise in the measured D_γ/D_α intensity ratio (Fig. 5), which is used experimentally to indicate the onset of recombination [9–12], is well reproduced by the simulations. Note that the signals are averaged over the whole inner/outer divertor volume, i.e. over volumes where recombination dominates and volumes where excitation dominates, thus leading to a smaller increase in the D_γ/D_α ratio than would be obtained if only recombination dominated [9]. Despite this rise in the D_γ/D_α intensity ratio, the plasma volume recombination in the simulations remains small, with a total $f_{rec} = 3.6\%$ at the highest density (while $f_{rec} = 10\%$ in the inner and 2% in the outer divertor region). This result shows that a significant increase in D_γ/D_α ratio – mainly due to D_γ recombination emission – does not necessarily imply large plasma volume recombination.

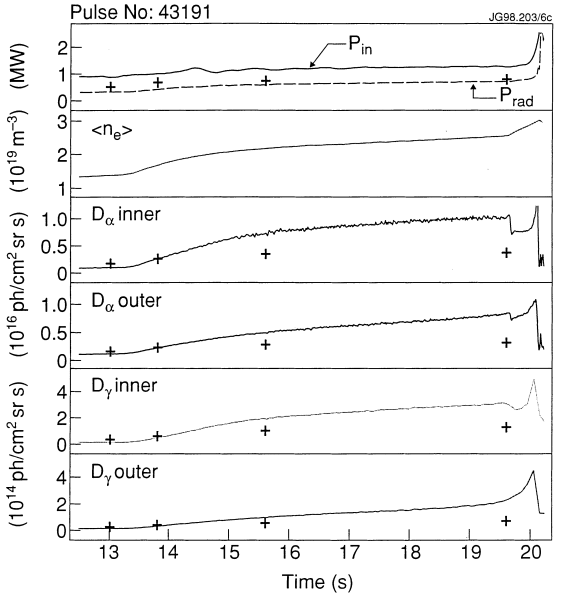

Fig. 4. Experimental traces and EDGE2D simulations with carbon impurities (+) for an Ohmic DL discharge in MarkIIA with vertical target configuration.

4. Effect of divertor plasma opacity on self-consistent 2D simulations

The measurements of Ly_β light reabsorption, although of modest degree, in the inner divertor of JET at high density provides sufficient ground for questioning

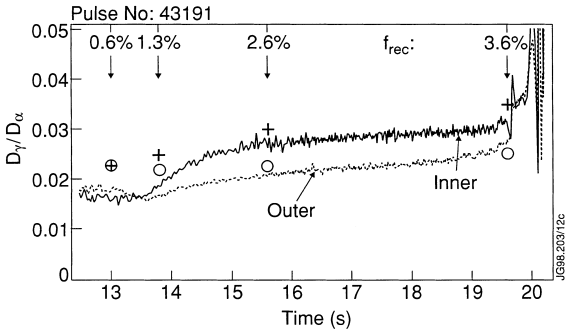

Fig. 5. Inner and outer divertor D_γ/D_α intensity ratios for the discharge of Fig. 4 and comparison with the EDGE2D simulations (+: inner, o: outer divertor). Also shown is the total number of recombination to ionization events, f_{rec}, for each simulation.

the assumption of optically thin divertor plasma used presently in 2D divertor transport codes. In this section we present our first attempt at including divertor plasma opacity corrections self-consistently in the EDGE2D/NIMBUS simulations of high density JET L-mode discharges. The aim of this study is twofold: to see if the measured optical thickness of the divertor plasma to Lyman radiation can be reproduced in the simulations and what are the modifications to the plasma parameters introduced by such corrections. To start with, this investigation requires the calculation of a new set of collisional-radiative rate coefficients for H (e.g. ionization, recombination and specific line emission rate coefficients) with opacity corrections. This is described in the following section.

4.1. Calculation of the H rate coefficients with optically thick corrections

Following Ref. [13], the optical thickness τ of a spectral line can be written as

$$\tau \propto n_l f_{l\to u}, \tag{4.1}$$

with n_l the number density of the lower level of the transition and $f_{l\to u}$ the absorption oscillator strength. The intensity ratio of two spectral lines originating from the same upper level, e.g. D_α and Ly_β, is given by

$$\frac{I(D_\alpha)}{I(Ly_\beta)} = \frac{g(\tau_{D_\alpha})A(D_\alpha)n_3}{g(\tau_{Ly_\beta})A(Ly_\beta)n_3}, \tag{4.2}$$

where I is the intensity, A the transition probability, $g(\tau)$ the escape factor of a spectral line ($g(\tau)=1$ for an optically thin transition) and n_3 the upper level of the transition. From the ratio of the optical thickness of the two lines,

$$\frac{\tau_{D_\alpha}}{\tau_{Ly_\beta}} = \frac{n_2 f_{2\to 3}}{n_1 f_{1\to 3}} = C, \tag{4.3}$$

we obtain

$$\tau_{D\alpha} = C\tau_{Ly_\beta}. \tag{4.4}$$

Thus, from Eqs. (4.2) and (4.4) and from the experimental measurements (see Section 1) we obtain in our case,

$$\frac{I(D_\alpha)/I(Ly_\beta)}{A(D_\alpha/A(Ly_\beta)} = \frac{g(C\tau_{Ly_\beta})}{g(\tau_{Ly_\beta})} = 1.3. \tag{4.5}$$

C is derived from the ratio of the oscillator strengths [14] and by running the ADAS collisional-radiative population code for H [15] to obtain the ratio of n_2/n_1. We start initially with the optically thin approximation and by assuming (n_e, T_e) = (10^{20} m^{-3}, 1 eV). This gives $C \ll 1$ and thus, from the curves in Ref. [16] we obtain $g(\tau_{D_\alpha})_y = 1$ (that is, the D_α line emission is optically thin). It follows from Eq. (4.5) that $g(\tau_{Ly_\beta}) = 0.77$ and thus, again using Ref. [16], the optical thickness of Ly_β is derived, $\tau_{Ly_\beta} = 0.38$. Note that these results are rather insensitive to the exact choice of n_e and T_e, as long as n_e is reasonably high and T_e is reasonably low, because of C still being $\ll 1$, implying $g(\tau_{D_\alpha}) = 1$. Using Eq. (4.1) we can then calculate escape factors for all Lyman series spectral lines, obtaining e.g. for Lyman-α $g(\tau_{Ly_\alpha}) = 0.29$. Note that for this initial investigation we assume angle-averaged escape factors, that is uniform opacity of the divertor plasma. At this stage, iteration of the H population calculation with the found Lyman light reabsorption is required until convergence is reached. In reality one iteration is sufficient since the opacity corrections do increase the ratio n_2/n_1, but C remains $\ll 1$ and therefore $g(\tau_{Ly_\beta})$ remains unchanged.

By rerunning the population code we have thus obtained a new data set of collisional-radiative rate coefficients for hydrogen, which include Lyman radiation reabsorption at all values n_e and T_e. With reference to the EDGE2D simulations, we establish the region of (n_e, T_e) space which overlaps with the region of high neutral density $n(D^0)$ in the divertor: $n_e \geqslant 10^{19}$ m^{-3} and $T_e \leqslant 5$ eV. We then merge the optically thin and optically thick H data sets, obtaining one with optically thick corrections for $n_e \geqslant 10^{19}$ m^{-3}, $T_e \leqslant 5$ eV which can be used in the 2D codes.

4.2. Effect of opacity on DI emission and plasma solution

The high density EDGE2D simulation of Section 3.2 is repeated using the optically thick H rate coefficients. D_α and Ly_β emission profiles obtained from the two simulations are compared in Fig. 6 (such measurements are not available for this particular discharge). The D_α emission increases by 20%, while the Ly_β emission is unchanged in going from the optically thin to optically thick case. The decrease in Ly_β/D_α ratio – with respect to the optically thin case – is ~20%, close to the experimentally measured values in the inner divertor at high density in similar pulses in MarkI. The reason for opacity effects of similar magnitude in inner and outer divertor is due to the almost symmetric detachment of the two divertor legs in the simulations with the present assumptions on cx momentum losses, as explained in Section 3.1.

Comparison of $n(D^0)$, n_e and T_e profiles in the region of the inner divertor where opacity corrections apply shows a small (10–20%) increase in $n(D^0)$ and n_e in the optically thick case, while T_e is unchanged. This is mainly due to the higher ionization rate coefficient (S_{iz}) obtained in the optically thick case, where the population density ratio n_2/n_1 is enhanced with respect to the optically thin case. For example, S_{iz} increases by a factor of 1.4 for (n_e, T_e) = (10^{20} m^{-3}, 1 eV). These variations in the plasma parameters, consistent with the modest opacity corrections, explain the small increase in D_α

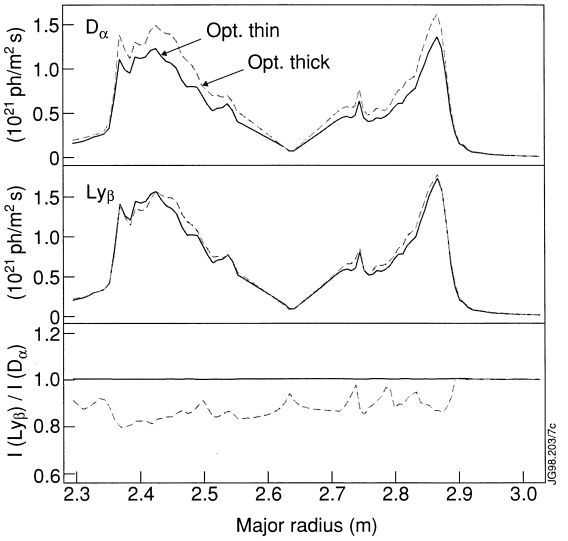

Fig. 6. Comparison of D_α and Ly_β divertor emission profiles from EDGE2D simulations for optically thin (solid traces) and thick (dashed traces) cases. The bottom panel shows the reduction in Ly_β/D_α intensity ratio in the optically thick solution (normalized to the optically thin value).

emission from the optically thin to thick simulation. In the case of Ly_β, the increase in $n(D^0)$ and n_e essentially compensates for the reduction in the escape factor ($g(\tau_{Ly_\beta})$ is reduced from 1 to 0.77), which results in no change to the Ly_β emission in the two simulations.

The modest enhancement to the divertor D_α emission obtained in the simulations when opacity corrections are included are not sufficient to explain the discrepancy with the measurements at high density. However, since full detachment cannot be achieved at present with EDGE2D/NIMBUS it is possible that the results presented in this section underestimate the overall effect of opacity in the inner divertor.

5. Conclusions

The continuous increase of divertor D^0 emission with rising plasma density, which is measured in JET Ohmic and L-mode DL divertor discharges, is not reproduced quantitatively by the EDGE2D/NIMBUS simulations (discrepancies of a factor of $\sim$3 are found at high density). The experimental increase in D_γ/D_α intensity ratio with rising density, which is shown to coincide with divertor detachment, is reproduced in the simulations and is mainly due to substantial D_γ recombination emission. This result is obtained despite the ratio of plasma volume recombination to ionization being small.

The asymmetry between inner and outer divertor detachment found in experiment, with detachment occuring at lower line averaged densities in the inner divertor, is found to be sensitive on the assumptions made for the calculation of the cx momentum losses. Reduction of the total ion flux to the inner divertor target from its peak value – measured experimentally close to the density limit – is not achieved with weak cx momentum losses, even if significant volume recombination takes place in the inner divertor region. This may indicate that strong volume recombination alone is not sufficient to attain complete divertor plasma detachment, but that strong cx losses and strong volume recombination are necessary simultaneously.

Measurements of Ly_β/D_α intensity profiles across the divertor at high density show signs of optical thickness of the inner divertor plasma to Lyman radiation. A first attempt at including such opacity corrections in the selfconsistent EDGE2D/NIMBUS plasma/impurity solution is presented. The modifications introduced by these corrections to the main plasma parameters are small, consistent with the modest Lyman radiation reabsorption observed experimentally. In particular, the enhancement in D_α emission (20–30%) is not sufficient to reconcile the discrepancies between experiment and simulations at high density.

Solution of present difficulties in EDGE2D/NIMBUS in reproducing the plasma detachment observed in JET L-mode DL discharges may result in better agreement with the experimental D^0 line emissivities at high density. In particular, this could imply that the opacity corrections obtained at present in the simulations may be underestimated.

References

[1] R. Simonini et al., Contrib. Plasma Phys. 34 (1994) 368.
[2] C.F. Maggi et al., J. Nucl. Mater. 241–243 (1997) 414.
[3] L.D. Horton et al., Studies in JET divertors of varied geometry I: non seeded plasma operation, Nucl. Fusion, 1998, accepted.
[4] T. Lovegrove et al., Plasma Phys. Control. Fusion, Proc. 22nd EPS Conf., 1995, III-301.
[5] G.C. Vlases et al., these Proceedings.
[6] A. Loarte et al., Nucl. Fusion 38 (1998) 331.
[7] K. Borrass et al., Plasma Phys. Control. Fusion, Proc. 24th EPS Conf., 1997, IV-1465.
[8] A.V. Chankin, J. Nucl. Mater. 241–243 (1997) 199.
[9] G. McCracken et al., Nucl. Fusion 38 (1998) 619.
[10] D. Lumma et al., Phys. Plasmas 4 (1997) 2555.
[11] J.L. Terry et al., Phys. Plasmas 5 (1998) 1759.
[12] R.C. Isler et al., Phys. Plasmas 4 (1997) 2989.
[13] R.W.P. McWhirter, in: R.H. Huddlestone, S.L. Leonard (Eds.), Plasma Diagnostic Techniques, Academic Press, New York, 1965, p. 201.
[14] W.L. Wiese et al., Atomic Transition Probabilities, NSRDS-NBS 4, 1966.
[15] H.P. Summers, ADAS, JET-IR (94)06 (1994).
[16] J.G. Doyle, R.W.P. McWhirter, MNRAS 193 (1980) 947.